

Investigation on Electrode Erosion Mechanism of Multi-Phase AC Arc by High-Speed Camera Observation

M. Tanaka¹, T. Ikeba¹, Y. Liu¹, S. Choi¹ and T. Watanabe^{1,2}

¹Dept. Environmental Chemistry and Engineering, Tokyo Institute of Technology, Yokohama, Japan

²Dept. Chemical Engineering, Kyushu University, Fukuoka, Japan

Abstract: A multi-phase AC arc plasma has been applied in the glass melting technology as a promising heat source. In this work, the high-speed camera system with appropriate band-pass filters was applied to measure the electrode temperature synchronized with vapor observation. Result shows the droplet ejection was contributed to the high electrode erosion of the multi-phase arc in the case of lower shield gas flow.

Keywords: Thermal Plasma, Multi-Phase AC Arc, Electrode Erosion, High-Speed Camera

1. Introduction

An innovative in-flight glass melting technology with thermal plasmas was developed to solve the problems of the conventional glass melting system [1, 2]. The granulated raw material with small diameter is injected into thermal plasmas and the powders contact fully with the plasma and/or burner flame. The high heat-transfer and temperatures of the plasma will melt the raw materials quickly. In addition, the decomposed gases of carbonates are removed during the in-flight treatment to reduce the refining time considerably. Compared with the traditional glass production, the total vitrification time is evaluated as only 2-3 h at the same productivity as the fuel-fired melter.

Arc plasmas as an energy source with high energy efficiency have been applied to the in-flight glass production. In particular, the multi-phase AC arc is one of the most suitable heat sources for the in-flight glass melting because it possesses many advantages such as high energy efficiency, large plasma volume (about 100 mm in diameter), low velocity (5-20 m/s) [3, 4]. In spite of the recent experimental efforts [5, 6], the multi-phase AC arc remains to be explored. In particular, the electrode erosion is one of the most considerable issues for the practical use of the multi-phase arc in glass melting process, because it determines the electrode lifetime and the purity of the products.

Combination of the two-color pyrometry and the high-speed camera observation was applied to measure the temperature of the electrode on the millisecond time scale [7]. Furthermore, the high-speed observations of the vapors in the arc were conducted to understand the dynamic behavior of the metal vapor, which indicated that the ambient oxygen is entrained into the arc more easily with increasing the number of the phases [8]. The objective in this work is to measure the electrode temperature synchronized with the electrode metal vapor observation by using the combination of the two high-speed camera systems. This study provides

important information to understand the erosion mechanism of the electrode in the multi-phase AC arc.

2. Experimental Procedure

2.1. Experimental setup and measurements system

The schematic diagram of the experimental setup and the synchronized measurement systems with two high-speed cameras is shown in **Fig. 1 (a)**. It consisted of 12 electrodes, arc chamber, and AC power supply. The electrodes were made of tungsten (98 wt%) and thoria (2 wt%) with diameter of 6 mm. The electrodes were divided into two layers, upper six and lower six electrodes. The upper electrodes were positioned at an angle of 30 degree with regard to the horizontal plane, while the lower electrodes were at an angle of 5 degree to control the plasma volume and the stability. The high-speed camera (FASTCAM SA-5, Photron) systems with appropriate band-pass filters were applied to measure the electrode temperature from the side of the chamber. The vapor observation synchronized with temperature measurement was conducted by the same type of camera which was installed above the chamber.

Figure 1 (b) shows the cross sectional view of the electrodes, which were symmetrically arranged by the angle of 30 degree. Because the melting point of the tungsten oxides is lower than that of metal tungsten, 99.99% argon was injected around the electrode as the shield gas to prevent them from the oxidation. In this work, the shield gas flow rate was changed from 2 to 5 L/min to investigate the electrode erosion mechanism.

2.2. Temperature measurements by high-speed camera

The implementation of two-color pyrometry for electrode temperature measurement involves the use of high-speed camera which was located beside the chamber. Spectroscopic measurements (iHR550, Horiba Jobin Yvon) were conducted to determine appropriate wavelengths for two-color radiations. High-speed video

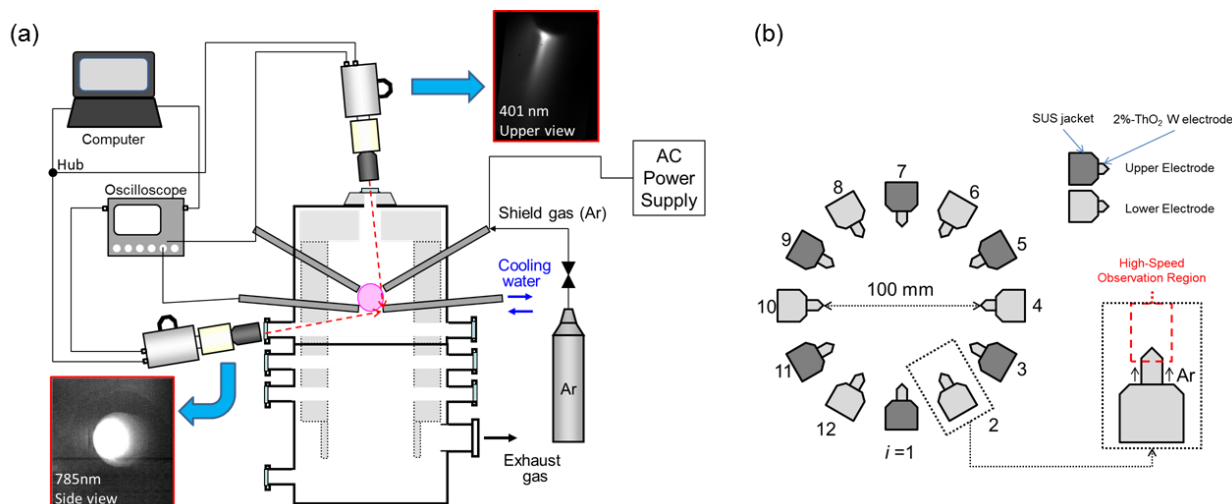


Fig. 1 Schematic diagram of experimental setup (a) and its cross sectional view (b).

camera with the band-pass filter system (MSI-2, Photron) was used to measure the radiation intensities as shown in **Fig. 2**. According to our previous work, two wavelengths, 785 ± 2.5 nm and 880 ± 5 nm, were selected for the temperature measurement in order to avoid the direct plasma emission. Frame rate and exposure time of the measurements were 5000 fps and 18 μ s, respectively. The voltage of each electrode was recorded at 1MHz by an oscilloscope (Scope Corder DL 850, Yokogawa) synchronized with the high-speed camera.

2.3. High-speed observations of vapors in the arc

The dynamic behavior of the vapors in the arc was investigated by using the same system with the temperature measurements. Emissions from argon and tungsten vapors were observed at the wavelengths of 738 ± 1.5 nm and 401 ± 0.5 nm, respectively. The camera was set at the frame rate of 5000 fps with the exposure time of 199.77 μ s.

3. Results and Discussion

Figure 3 shows the waveforms of the arc current and voltage synchronized with the high-speed camera observation in the 12-phase arc at 2 L/min of the shield gas flow rate. While **Fig. 4** shows the representative high-speed images of the 12-phase arc for tungsten vapor, argon vapor, and the electrode during one AC cycle. Upper and middle images show the emission from tungsten and argon, respectively. Bottom images correspond to the thermal emission from the electrode surface at 785 nm, which was selected to measure the temperature as well as 880 nm. The indicated time in Fig. 4 corresponds to the time in Fig. 3. Thus, the electrode was at anodic period in the first half period, while at the cathodic period in the other half. The strong tungsten emission separated from other emissions was successfully

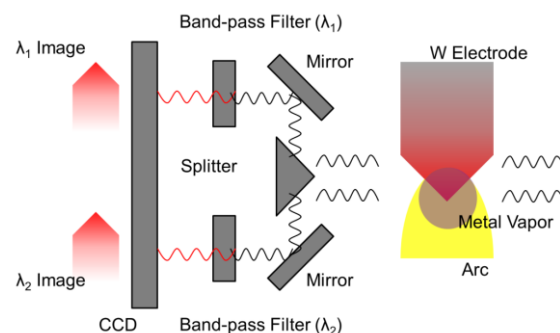


Fig. 2 Schematic diagram of the combination of the high-speed video camera and the band-pass filters.

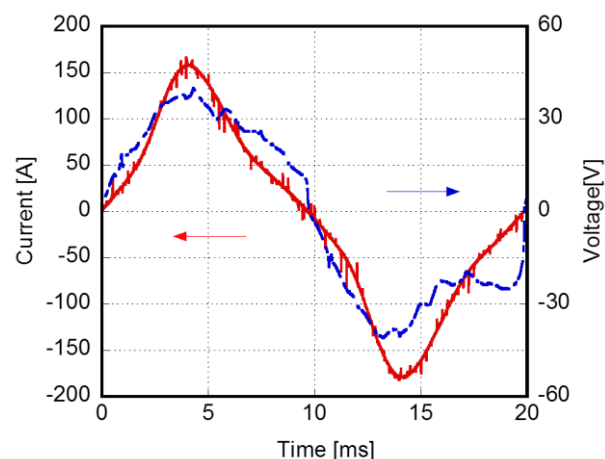


Fig. 3 Representative waveforms of the arc current and voltage in the 12-phase arc.

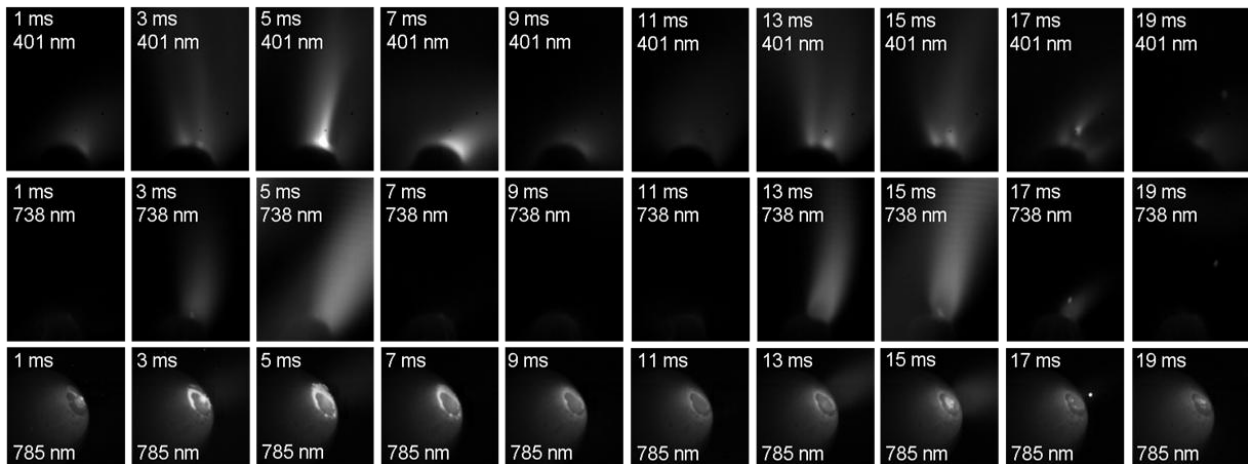


Fig. 4 Representative snapshots of high-speed camera images; upper column: tungsten emission at 401 nm, middle: argon emission at 738 nm, bottom: thermal radiation from the electrode surface at 785 nm.

observed by using the high-speed camera system with appropriate band-pass filters. Obtained snapshots indicate that the tungsten electrode started to evaporate at 5 ms in the anodic period. The reason for this result is the larger heat transfer at the anodic period compared with that at the cathodic period, resulting from the electron condensation.

The relative intensity of tungsten emission to argon emission was calculated to evaluate the number density of the tungsten vapor qualitatively. **Figure 5** shows the snapshots and distributions of the relative intensity of tungsten emission to argon emission at 5 ms in the anodic period for different flow rate of argon gas. At this time, the tungsten evaporation was mainly observed in the anodic period. In addition, the relative intensity at 2 L/min of shield gas flow rate is considerably higher than that at 5 L/min.

Figure 6 shows the temperature distribution of the electrode surface at 5 ms in the anodic period for different shield gas flow rate. The surface temperature of electrode tip at 2 L/min is higher than that at 5 L/min. The maximum temperature and the molten area were evaluated from these results. The molten area was defined as the area where the temperature was more than the melting point of tungsten. **Figure 7** shows the maximum temperature and the molten area of the electrode surface in the 12-phase arc for different flow rate of the shield gas. The temperature at 2 L/min of shield gas flow rate was higher than that at 5 L/min. While the molten area on the electrode surface at 2 L/min was smaller than that at 5 L/min. These results show the good agreement with the synchronized vapor observation. This is because the arc in the case with 2 L/min was more constricted due to the larger evaporation of the electrode. Then, the arc spot in the case of 2 L/min was stabilized compared with that of 5 L/min. Consequently, the electrode erosion in the case

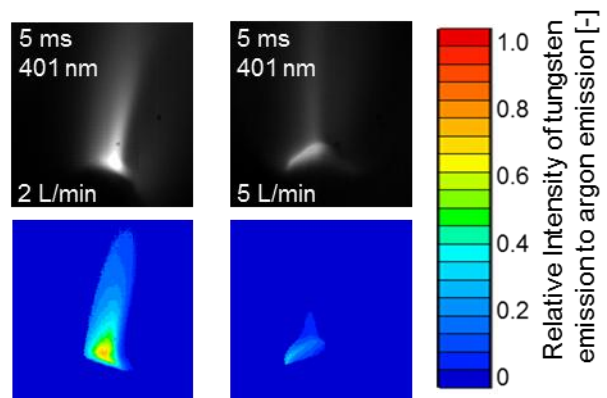


Fig. 5 High-speed images and distributions of the relative intensity of tungsten emission to argon emission at 5 ms in the anodic period for different argon gas.

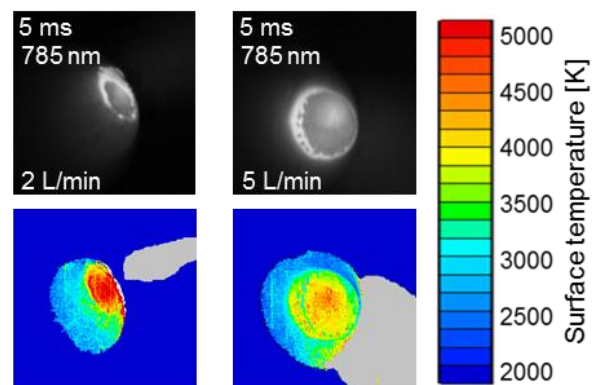


Fig. 6 Temperature distribution of the electrode surface at 5 ms in the anodic period for different shield gas flow rates.

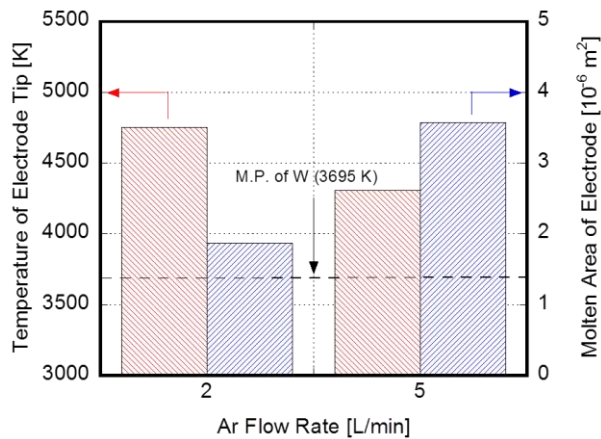


Fig. 7 Maximum temperature of electrode tip and the molten area of electrode at different shield gas flow rates.

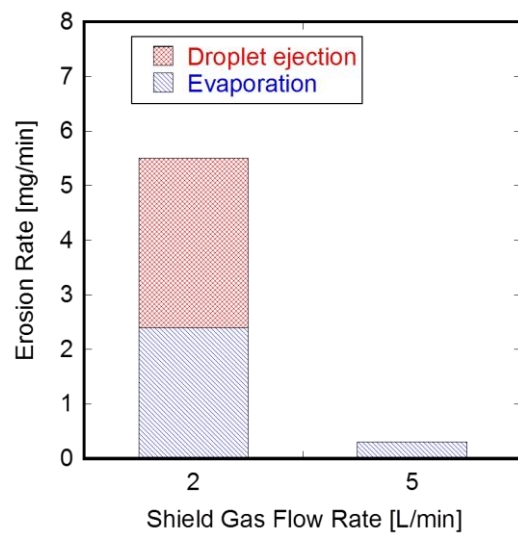


Fig. 8 Relationship between the erosion rate and the shield gas flow rate.

of 2 L/min becomes severer than that of 5 L/min due to the increase of temperature of electrode tip.

Moreover, the droplet ejection from the molten electrode surface was observed at 17 ms in the cathodic period, as shown in Fig. 4. In order to evaluate the amount of the droplet ejection, the number of the droplets was counted during the three AC periods. **Figure 8** shows the relationship between the erosion rate and the shield gas flow rate. In the case of 5 L/min of the shield gas flow rate, the electrode was eroded only by the evaporation. Contrastingly, the electrode was eroded by both the evaporation and the droplet ejection in the case of the 2 L/min. This should be related to the entrainment of ambient oxygen gas in the case of lower shield gas flow rate. Consequently, the evaporation rate was increased, resulting in the arc constriction. Mechanism of the droplet ejection in the case of lower shield gas flow is currently under investigation.

4. Conclusion

The measurement of the electrode temperature synchronized with the metal vapor observation has been successfully conducted for the first time. Obtained remarks are as follows.

1) The strong tungsten emission separated from the other emissions was observed at the anodic period in the case of lower argon gas flow rate. The synchronized temperature measurements revealed that the electrode tip temperature increased with decreasing the argon gas flow rate. This is because the discharge point was stabilized due to the constriction of arc in anodic period at the lower flow rate of shield gas.

2) The droplet ejection from the molten electrode surface was observed in the case of 2 L/min of the shield gas flow rate. The droplet ejection was contributed to the high electrode erosion of the multi-phase arc. This study provides important information to understand the erosion

mechanism of the electrode, which will improve the practical development of multi-phase AC arc.

5. Acknowledgements

The financial support provided by the Strategic Development of Energy Conservation Technology Project of NEDO (New Energy and Industry Technology Development Organization, Japan) is gratefully acknowledged.

Mr. Kosaku Saito (Photron) is also acknowledged for his help to establish the system with the high-speed cameras.

6. References

- [1] Y. Yao, T. Watanabe, T. Yano, T. Iseda, O. Sakamoto, M. Iwamoto and S. Inoue, *Science and Technology of Advanced Materials*, **9**, 025013 (2008).
- [2] T. Watanabe, K. Yatsuda, Y. Yao, T. Yano and T. Matsuura, *Pure and Applied Chemistry*, **82**, 1337 (2010).
- [3] Y. Liu, Y. Tsuruoka, M. Tanaka, T. Ichihashi, T. Yano and T. Watanabe, *Thin Solid Films*, **519**, 7005 (2011).
- [4] M. Tanaka, Y. Tsuruoka, Y. Liu and T. Watanabe, *IOP Conference Series: Material Science and Engineering*, **18**, 112010 (2011).
- [5] M. Tanaka, Y. Tsuruoka, Y. Liu, T. Matsuura and T. Watanabe, *IEEE Transactions on Plasma Science*, **39**, 2904 (2011).
- [6] M. Tanaka, Y. Tsuruoka, Y. Liu, T. Matsuura and T. Watanabe, *Current Applied Physics*, **11**, S35 (2011).
- [7] M. Tanaka, T. Ikeba, Y. Liu, T. Matsuura and T. Watanabe, *Journal of Physics: Conference Series*, **406**, 012008 (2012).
- [8] M. Tanaka, T. Ikeba, Y. Liu, S. Choi and T. Watanabe, *Journal of Physics: Conference Series*, **441**, 012015 (2013).